Lasing and Spectroscopic Characteristics of a New Nd Laser Crystal – Strontium Fluorovanadate

P. Hong, X. X. Zhang, G. Loutts, R. E. Peale, H. Weidner, M. Bass, and B. H. T. Chai

Center for Research and Education in Optics and Lasers (CREOL), University of Central Florida, 12424 Research Parkway, Orlando, Florida 32826

S. A. Payne, L. D. DeLoach, L. K. Smith, W. F. Krupke

Lawrence Livermore National Laboratory, University of California, Livermore, California 94550

Abstract

High slope efficiency and low threshold lasing at 1.065 μm has been achieved in Nd^{3+}:$Sr_5(VO_4)_3F$. The presence of more than two inequivalent sites for Nd^{3+} in this crystal was demonstrated. Spectroscopic properties and their effect on the lasing performance are reported.

Introduction

As high power laser diodes become more readily available, there is a need to further improve solid state laser media for both high slope efficiency and low threshold operation. We report here a newly discovered promising laser crystal, Nd^{3+}:$Sr_5(VO_4)_3F$ (or Nd^{3+}:SVAP).

SVAP is isomorphous to calcium fluorapatite ($Ca_5(PO_4)_3F$ or FAP) [1] which is hexagonal with space group $P6_3/m$ and unit cell dimensions of a_0=10.0077 Å , c_0=7.4342 Å . Each unit cell contains two $Sr_5(VO_4)_3F$ molecules. Two non-equivalent Sr^{2+} sites, M_I (40%, 9-fold with C_3 symmetry) and M_{II} (60%, 7-fold with C_{1h} symmetry), exist in each unit cell. Since the M_{II} site has one F^- in coordination, it is the dominant site for rare earth substitution, although a small fraction of dopant ions substitute in the M_I site. An Nd^{3+} ion substitutes for an M_{II} Sr^{2+} ion in the structure with the unbalanced charge compensated by replacing F^- with O^{2-} [2]. High quality single crystals were grown by conventional Czochralski pulling in our crystal growth laboratory. The growing conditions are similar to those used to grow the isomorph, FAP [3, 4].

Laser performance

An Nd^{3+}:SVAP crystal was cut with flat and parallel faces containing the c axis and anti-reflection (AR) coated from 1.0 to 1.1μm. The laser resonator was composed of a 5 cm radius curvature reflector (high reflectivity at 1.0-1.1μm and high transmission at 790-810 nm) and a flat output coupler (OC) with transmission up to 5%. The pumping light was focused with a 10 cm focal length lens through the HR mirror into the crystal. Both pulsed and cw laser-pump-laser experiments were performed simulating diode laser pumping. Pulsed lasing was achieved with a long pulsed Cr:LiSrAlF (Cr:LiSAF) laser which was tuned to the Nd^{3+}:SVAP absorption peak at 810 nm and has a spectral bandwidth about 1 nm. CW lasing was achieved with a cw Ti:sapphire laser tuned to 810 nm with spectral bandwidth about 0.1 nm. Lasing from the Nd^{3+}:SVAP $^4F_{3/2} \rightarrow {}^4I_{11/2}$ transition at 1.065 μm is linearly polarized along the c-axis (π-polarization).

A 3.8 mm long, 0.26 at.% Nd^{3+}:SVAP crystal was tested for laser performance. About 85% of the long pulsed pumping energy and 98% of cw pumping power were absorbed. The thresholds and slope efficiencies for both pulsed and cw operation at 1.065 μm are listed in Table 1. With a 5% output coupler, a slope efficiency of 62% and 49.4% was obtained in pulsed and cw operation respectively. Higher slope efficiency is expected with a higher transmission output coupler [5].

The loss present in laser operation can be derived from the slope efficiency obtained in the cw laser-pump-laser experiment. A plot of the inverse slope efficiency against the inverse output coupler transmissions gives an intrinsic slope efficiency of

OSA Proceedings on Advanced Solid-State Lasers, 1994, Vol. 20
Tso Yee Fan and Bruce H. T. Chai (eds.)

67% and a double-pass passive loss of 1.5% for cw operation through the following relation [6]

$$1/\eta = 1/\eta_0 + (L/\eta_0)(1/T) \quad (1)$$

where η is the measured slope efficiency, η_0 is the intrinsic slope efficiency, T is the transmission of the output coupler, and L is the double-pass passive loss.

A 1.3 mm long 0.65 at.% Nd^{3+} doped SVAP crystal was also tested for laser performance in the same cavity. Only 22% slope efficiency was obtained with a 5% output coupler in cw operation, which is due to concentration quenching as shown below.

Table 1. Thresholds and slope efficiencies of Nd^{3+}:SVAP lasing at 1.065 μm in pulsed and cw operation.

	pulsed		cw	
T (%)	threshold (μJ)	slope efficiency (%)	threshold (mW)	slope efficiency (%)
1.2	3.6	38.2	5.8	28.6
3	5.2	59.2	9.4	43.4
5	6.0	62.0	13.2	49.4

Spectroscopic properties

The spectroscopic properties of Nd^{3+}:SVAP were studied in several samples. The Nd doping concentration in the melt were 0.2, 1, 1.5, 2, 3, and 4 at.%. Using microprobe analysis, the actual Nd concentration in the grown crystals were found to be 0.05, 0.26, 0.38, 0.48, 0.63 and 0.71 at.%, respectively. The distribution coefficient is different for different doping levels, decreasing as the Nd doping level increases.

Polarized transmission spectra of the $^4I_{9/2} \rightarrow {}^4F_{3/2}$ transition at 2 K are shown in Fig. 1 and emission spectra of the $^4F_{3/2} \rightarrow {}^4I_{11/2}$ transition at 20 K when pumped by a multi-line argon ion laser are shown in Fig. 2. Two lines in the transmission and six lines in the emission spectrum are expected for a Nd^{3+} ion in a single site crystal at these temperatures. In SVAP, it seems that Nd^{3+} ions are in more than two different environments as seen in Figs. 1 and 2. As the Nd^{3+} concentration increases, the absorption coefficients of the lines in the middle of the $^4I_{9/2} \rightarrow {}^4F_{3/2}$ absorption spectra decrease relatively to the strong lines on the sides.

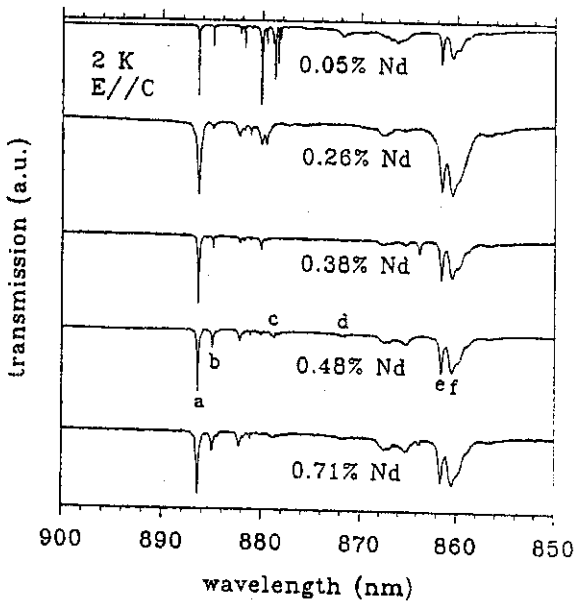

Fig. 1. Transmission spectra ($^4I_{9/2} \rightarrow {}^4F_{3/2}$) of Nd^{3+}:SVAP at 2 K for different Nd^{3+} concentrations.

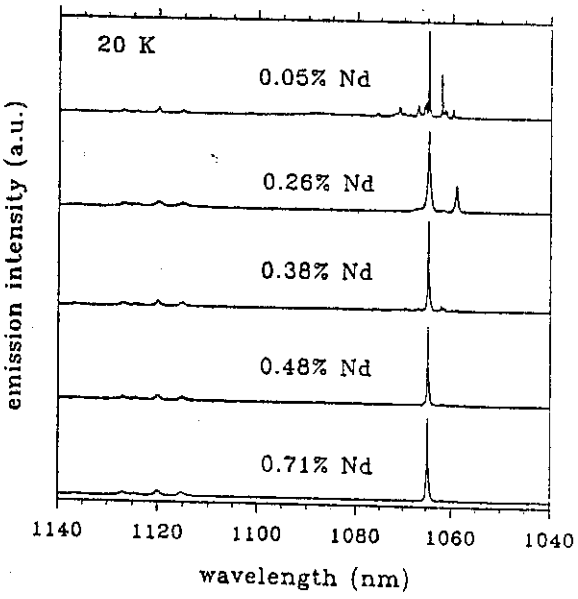

Fig. 2. Emission spectra ($^4F_{3/2} \rightarrow {}^4I_{11/2}$) of Nd^{3+}:SVAP at 20 K, excited by a multi line argon ion laser, for different Nd^{3+} concentrations.

In order to understand these multi line absorption and emission of Nd^{3+}:SVAP, we conducted a site selective excitation spectroscopy study with a 0.48% Nd doped SVAP sample using a tunable Ti:sapphire laser.

As shown in Fig. 3 (a), when the sample was excited at the peak of line a (886.4 nm) in Fig. 1, only

one strong emission line was observed with its center at 1.065 μm. When excited at line e and f, the same spectra were obtained as when we excited with line a, indicating that line e and f are either from the same origin or strongly coupled to this emission. However, the energy separation between line a and line f matches that between the 1.065 μm emission line and its thermal replica at high temperature as we will see later. We therefore assign line a and line f as the split sublevels of the $^4F_{3/2}$ manifold in a particular site. We further attribute this site to the main site, M_{II} site, since its absorption and emission are the strongest observed.

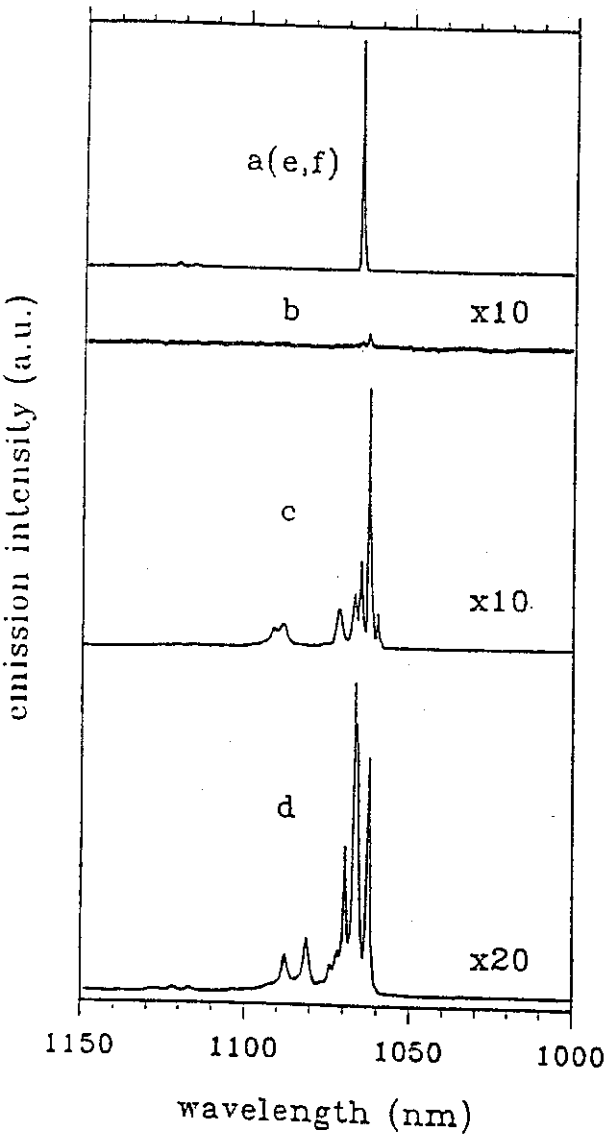

Fig. 3. Emission spectra ($^4F_{3/2} \rightarrow {}^4I_{11/2}$) of 0.48 at% Nd^{3+}:SVAP at 15 K when excited at (a) 886.4 nm, (b) 885.0 nm, (c) 879.8 nm, and (d) 871.6 nm.

Excitation at line b in Fig. 1 resulted in a weak emission at a wavelength of 1.063 μm, see Fig 3(b). For excitation at absorption lines between line b and e, many weak emission lines, including the main emission line, were detected. The relative intensity of these lines depends on the excitation wavelength applied as seen in Fig. 3(c) and (d). These absorption features are most probably due to M_I site and others that result from charge compensation, all of which we call secondary sites. The existence of the main emission line at 1.065 μm indicates that energy transfer takes place from the secondary sites to the main site.

More complicated site selective excitation spectra were observed. When excitation is at wavelengths off the absorption peaks weak emission lines are always detected. It seems that weak absorption lines cover the whole region in the absorption spectrum shown in Fig. 1. Detailed spectroscopic analysis will be presented elsewhere.

Room temperature transmission and emission spectra were measured and are shown in Figs. 4 and 5. As can be seen, at room temperature, there are only two strong absorption lines from the $^4I_{9/2} \rightarrow {}^4F_{3/2}$ transition. The absorption and emission of the secondary sites at room temperature are much weaker than at 2 K. Line e seen at low temperature also becomes weaker while line f remain relatively strong.

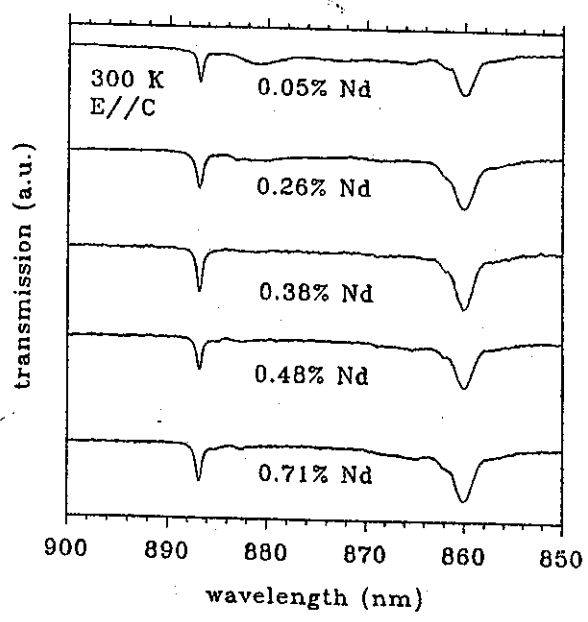

Fig. 4. Transmission spectra ($^4I_{9/2} \rightarrow {}^4F_{3/2}$) of Nd^{3+}:SVAP at 300 K for different Nd^{3+} concentrations.

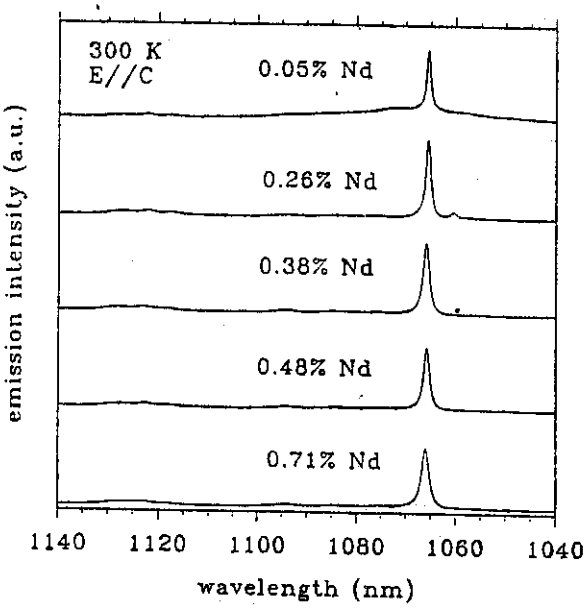

Fig. 5. Emission spectra ($^4F_{3/2} \rightarrow {}^4I_{11/2}$) of Nd^{3+}:SVAP at 300 K, excited by a multi line argon ion laser, for different Nd^{3+} concentrations.

The energy levels of the main M_{II} site given in Table 2 were determined from 80 K absorption and emission data. Because a multi line argon ion laser was used as excitation source, the crystal temperature is actually higher than 80 K. The Stark splitting of the $^4F_{3/2}$ level in Nd^{3+}:SVAP is 346 cm^{-1}. It is slightly smaller than those in Nd^{3+}:FAP and Nd^{3+}:SFAP (Nd^{3+}:$Sr_5(PO_4)_3F$).

Table 2. Energy levels of Nd^{3+} in the main site of SVAP

spectral term	wavenumber (cm^{-1})
$^4F_{3/2}$	11624, 11278
$^4I_{15/2}$	6620, 6506, 6396, 6373, 6311, 6257, 6246, 5716
$^4I_{13/2}$	4480, 4387, 4376, 4353, 4306, 4261, 3803
$^4I_{11/2}$	2484, 2410, 2391, 2357, 2319, 1889
$^4I_{9/2}$	667, 551, 499, 449, 0

The $^4F_{3/2}$ state of Nd^{3+}:SVAP has very strong self-absorption. To avoid decay time lengthening due to self-absorption, luminescence time decay measurements were carried out with fine-ground powders of crystals. At room temperature, the luminescence decay of the $^4F_{3/2}$ state is exponential for the very low concentration sample with a decay time of 213 μs. As the Nd concentration increases the decay becomes non-exponential with a shorter decay time. The decay time verses concentration at room temperature is listed in Table 3. For non-exponential decay a mean decay time is defined as

$$\tau = \frac{1}{I(0)} \int_0^\infty I(t)dt \qquad (2)$$

where I(0) and I(t) are the luminescence intensities at time 0 and t. The decrease of the decay time with increase in Nd concentration indicates the strong concentration quenching in this crystal.

Table 3. Decay time of the $^4F_{3/2}$ state of Nd^{3+}:SVAP as a function of concentration at 300 K

Nd^{3+} concentration (at.%)	decay time (μs)
0.05	213
0.26	171
0.38	156
0.48	124
0.63	116
0.71	80

The intrinsic laser slope efficiency depends on the quantum efficiency and the pump and lasing wavelengths in cw operation. For the same type of crystal, the difference of the intrinsic slope efficiencies in samples with different Nd^{3+} concentrations depend only on the quantum efficiencies [3]. In the presence of concentration quenching the quantum efficiency is equal to the ratio of the effective decay time to the radiative decay time. Therefore, for high concentration Nd^{3+}:SVAP crystals the laser slope efficiency will decrease due to concentration quenching. For 0.26 at.% Nd^{3+} doped SVAP crystal, the quantum efficiency is 80 % but for 0.63 at.% Nd^{3+} doped SVAP it is only 54%. Therefore, the expected slope efficiency of the 0.63 at.% Nd^{3+}:SVAP is lower than that of 0.26 at.% Nd^{3+}:SVAP as shown in our lasing test results.

Conclusion

In Nd doped SVAP crystal, Nd ions enter many inequivalent sites. From the spectroscopic properties they can be classified into two groups, main and secondary sites. The main site has much stronger absorption and emission than the secondary sites. It is the lasing site of this crystal. The secondary sites have very weak absorption and emission and the absorption lines seem to cover a wide spectrum. As temperature increases, the relative intensity of the secondary sites to the main site becomes weaker.

In summary, high slope efficiency and low threshold laser performance in both pulsed and cw operation were achieved at 1.065 μm in low concentration Nd^{3+}:SVAP. It has a linearly π-polarized narrow single line emission with a cross-section of 5×10^{-19} cm^2 and radiative lifetime 213 μs. However, the multi site nature and the strong lifetime quenching in this crystal may limit its wide utilization.

References:

1. D.A. Grisafe and F. A. Hummel, J. Solid State Chem. 2, 160 (1970).
2. R.C. Ohlmann, K.B. Steinbruegge, and R. Mazelsky, Applied Optics, 7(5), 905 (May 1968).
3. X.X. Zhang, G. B. Loutts, M. Bass, and B.H.T. Chai, Appl. Phys. Lett. 64, 10 (1994).
4. G. B. Loutts and B.H.T. Chai, SPIE Proc. 1863, 31 (1993).
5. S.A. Payne, B.H.T. Chai, W.L. Kway, L.D. DeLoach, L.K. Smith, G. Lutts, R. Peale, X.X. Zhang, G.D. Wilke, and W.F. Krupke, Conf. on Lasers and Electro-Optics (CLEO), Baltimore, (1993), post deadline paper.
6. J.A. Caird, S.A. Payne, P.R. Staver, A.J. Ramponi, L.L. Chase, and W.F. Krupke, IEEE J. QE 24, 1077 (1988).